



## Metal ions-triggered photo-induced fluorescence change in rhodamine B-based photo-responsive complexes

Yuanyuan Li <sup>a</sup>, Zining Feng <sup>a</sup>, Yajing Li <sup>a</sup>, Wenhui Jin <sup>a</sup>, Qiuchen Peng <sup>b</sup>, Panke Zhang <sup>b,\*</sup>, Juan He <sup>a</sup>, Kai Li <sup>b,\*</sup>

<sup>a</sup>*School of Chemistry and Chemical Engineering, Henan University of Technology, Henan 450001, P. R. China.*

<sup>b</sup>*College of Chemistry and Molecular Engineering, Zhengzhou University, Henan 450001, P. R. China. E-mail: likai@zzu.edu.cn.*

### Abstract

Photo-responsive materials with tunable properties by multiple stimuli have been widely used as molecular machines, molecular logic gates, optical data storages, etc. In this work, we report a rhodamine B-based photo-responsive system, whose properties could be facilely modulated by metal ions (Zn(II), Ni(II) and Hg(II)). These metal ions endow the complexes (**L-Zn**, **L-Ni** and **L-Hg**) with similar photochromic property but distinctly different photo-induced fluorescence change. Upon UV light irradiation, the spiro lactam ring in rhodamine B moiety turned from a close form to an open form, along with enlarged conjugated structure with intense absorbance. Interestingly, fluorescence “turn off”, “no change” and “turn on” responses were induced by Zn(II), Ni(II) and Hg(II) respectively upon UV light irradiation. Taking advantage of the prominently different characteristics caused by metal ions, different logic gates were designed by simply varying the inputs of metal ions and UV light. This work provided a new strategy for developing multifunctional photo-responsive materials, which were further beneficial for constructing photo-controlled logic gates with tunable performance.

**Keywords:** Photo-responsive; Rhodamine B; Metal ion; Fluorescence change; Logic gate

### 1. Introduction

Photo-responsive materials are a kind of materials which can undergo physical or

chemical transformations under light stimulation [1, 2]. Because of the light-controlled properties, photo-responsive materials have attracted wide attentions in constructing a variety of functional materials including molecular machines, molecular logic gates, optical data storages, fluorescence sensors, photo-controllable switches, etc [3-13]. Some multifunctional photo-responsive systems including azobenzene, spiropyran, spirooxazine, dithienylethene, viologen and anil are reported successively [14-19].

In recent years, great efforts have been made on combining various stimuli with light to endow photo-responsive materials with more abundant properties, which have become a hot topic for developing multifunctional photo-responsive materials. Up to now, the stimuli including pH, heat, electricity and mechanical force have been introduced to the development of multifunctional photo-responsive materials [20-27]. Metal ions, however, to the best of our knowledge, have been rarely reported as a kind of efficient stimulus in regulating photo-responsive performance. It is still a great challenge to develop metal-controlled photo-responsive systems with tunable performances.

Rhodamine B salicylaldehyde hydrazone metal complex, a more recently reported photo-responsive system, has the advantages of simple synthesis, distinct color change upon UV light irradiation, and good fatigue resistance [28-32]. Meanwhile, its metal complex structure makes it a good candidate and possible to regulate the photo-responsive property by metal ions. Therefore, in this work, 2,4-dihydroxybenzaldehyde rhodamine B hydrazone Schiff base (**L**) was chosen as ligand and attempts have been made to systematically regulate the photo-responsive performance by changing the types of metal ions (Table 1). Although the complexes (**L-M**) formed by **L** and metal ions (**M**) exhibited similar isomerization in the spiro lactam ring of rhodamine B moiety from a close form to an open form, they showed different photo-responsive properties upon UV light irradiation. Zn(II) can induced the absorbance change from nothing to an obvious value at 556 nm with a quenched fluorescence emission at 516 nm after UV light irradiation. Ni(II) caused similar absorbance change to that of Zn(II) after UV light irradiation but no

fluorescence was observed whether or not the complex was irradiated. For Hg(II), however, the properties were rather different. Both of the absorbance (556 nm) and fluorescence (589 nm) were significantly enhanced after UV light irradiation. Taking advantage of the prominently different characteristics caused by metal ions, different logic gates were facily designed by simply varying the inputs of metal ions and UV light.

**Table 1.** Fluorescence and absorption properties of **L** regulated by Zn(II), Ni(II) and Hg(II) before and after UV light irradiation.

	<b>Irradiation</b>	<b>L-Zn</b>	<b>L-Ni</b>	<b>L-Hg</b>
Fluorescence	Before	Strong	No	Weak
	After	Weak	No	Strong
Absorbance	Before	No	No	Weak
	After	Strong	Strong	Strong

## 2. Experimental

### 2.1. Materials

All the materials of analytical grade were used from the suppliers without further purification. Rhodamine B, benzoyl hydrazine, hydrazine hydrate and 2,4-dihydroxybenzaldehyde were ordered from J&K Chemical Co., Beijing, China. Zinc(II) nitrate hexahydrate, nickel(II) nitrate hexahydrate and mercury(II) perchlorate hydrate were purchased from Energy Chemical Co., Shanghai, China. All the other materials were supplied by Sinopharm Chemical Reagent Beijing Co., Beijing, China.

### 2.2. Apparatus

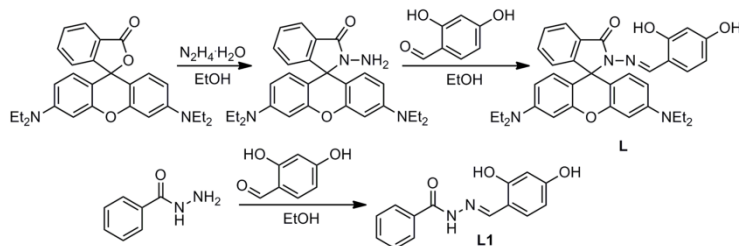
Fluorescence spectra were recorded on a JASCO FP-8300 spectrofluorimeter (1 cm quartz cell). Absorption spectra were determined on a JASCO V-750 spectrophotometer (0.2 cm quartz cells for **L-Zn** and **L-Ni** and 1 cm quartz cells for **L-Hg**). Electrospray ion mass spectrometry (ESI-MS) data were collected on an Agilent Technologies 6420 triple quadrupole LC/MS spectrometer without using the

LC part. The nuclear magnetic resonance (NMR) spectra were collected on a Bruker 600 Avance NMR spectrometer. UV light of 365 nm was produced by a Qiwei WFH-204B hand-held ultraviolet lamp. All the photos were carried by a Nikon D5500 camera.

### 2.3. Syntheses

**Syntheses of L:** The synthetic route for **L** was shown in Scheme 1 [33]. Rhodamine B hydrazide was prepared with rhodamine B (8 mmol, 3.54 g) and hydrazine hydrate (85%) by refluxing in 30 mL ethanol for 6 h [34]. Then rhodamine B hydrazide (4 mmol, 1.83 g) was dissolved in 60 mL absolute ethanol. After that 2,4-dihydroxybenzaldehyde (5 mmol, 0.69 g) was added dropwise with vigorous stirring. The mixture was heat to 80 °C and refluxed overnight. After that, the solvent was concentrated to about 15 mL under reduced pressure, followed by standing at 4 °C overnight to form a pink precipitate. After being filtered, the precipitate was washed with 50 mL absolute ethanol for three times. The resulting precipitate was finally dried under reduced pressure to yield a pink solid (1.50 g, yield 65%). <sup>1</sup>H NMR (600 MHz, DMSO-*d*<sub>6</sub>)  $\delta$  (ppm): 10.54 (s, 1H), 9.02 (s, 1H), 7.89 (s, 1H), 7.56 (m, 2H), 7.09 (s, 1H), 6.35 (m, 8H), 6.18 (s, 1H), 3.30 (q, 8H), 1.07 (t, 12H). <sup>13</sup>C NMR (151 MHz, DMSO-*d*<sub>6</sub>)  $\delta$  (ppm): 163.60, 161.61, 159.95, 153.24, 152.97, 151.35, 148.99, 134.12, 132.19, 129.51, 129.28, 128.19, 124.27, 123.35, 111.02, 108.63, 108.34, 105.41, 103.09, 97.81, 65.94, 44.13, 12.87.

**Syntheses of 2,4-dihydroxybenzaldehyde benzoyl hydrazine Schiff base (L1):** Benzoyl hydrazine (4 mmol, 0.54 g) and 2,4-dihydroxybenzaldehyde (4 mmol, 0.55 g) were dissolved in 60 mL absolute ethanol. The mixture was heat to 80 °C and refluxed for 30 min. After that, the solvent was cooled to room temperature and then filtered. Precipitate was collected and washed with 50 mL absolute ethanol for three times. After drying under reduced pressure, a pink solid (0.83 g, yield 81%) was obtained. <sup>1</sup>H NMR (600 MHz, DMSO-*d*<sub>6</sub>)  $\delta$  (ppm): 11.96 (s, 1H), 8.54 (s, 1H), 7.95 (d, 2H), 7.60 (t, 1H), 7.54 (t, 2H), 7.32 (d, 2H), 6.39 (m, 2H). <sup>13</sup>C NMR (151 MHz, DMSO-*d*<sub>6</sub>)  $\delta$  (ppm): 163.01, 161.27, 160.04, 149.77, 133.49, 132.26, 131.87, 128.97, 128.03, 110.99, 108.20, 103.19.



**Scheme 1.** Synthetic route of **L** and **L1**.

#### 2.4. Preparation of the complexes of **L-Zn**, **L-Ni** and **L-Hg**

Stock solutions of Zn(II), Ni(II) and Hg(II) were prepared from their nitrate salts or perchlorate salts of analytical grade in doubly distilled deionized water. Stock solution of **L** was prepared in tetrahydrofuran. Solutions of **L-Zn**, **L-Ni** and **L-Hg** were prepared by adding 10 equiv. of the corresponding metal salts separately to the solution of **L** to ensure **L** can convert to complexes adequately.

### 3. Results and discussion

#### 3.1. The bonding mode of **L** with metal ions

To get insight into the bonding mode of different metal ions with **L**, UV-vis titration experiments were carried out. As shown in Fig. 1, all of the metal ions of Zn(II), Ni(II) and Hg(II) can cause increased absorbance of **L** in visible region. The absorption bands centered at around 410 nm, 421 nm and 558 nm, respectively. Isosbestic points were observed in all the spectra after the titration experiments, which suggested that new compounds have been formed between the ligand and Zn(II), Ni(II) and Hg(II) (**L-Zn**, **L-Ni** and **L-Hg**). Moreover, the metal-to-ligand ratios could be obtained from the absorbance titration data of the metal ions and **L** based on the following equation [35, 36]:

$$\log\left(\frac{A-A_0}{A_{\max}-A}\right) = \log K + n \log[M] \quad (1)$$

where  $A$  is the absorbance of ligand as a function of the addition of metal ions,  $A_0$  represents the absorbance of ligand without metal ions and  $A_{\max}$  is the absorbance of ligand with excess amount of metal ions.  $K$  represents the association constant and  $n$  is the stoichiometry of the complex between ligand and metal ions, respectively.  $[M]$  stands for the concentrations of metal ions. As shown in the insets of Fig. 1(b), Fig.

1(d) and Fig. 1(f), excellent linear relationships could be obtained between  $\log[(A-A_0)/(A_{\max}-A)]$  and  $\log[M]$  ( $R^2 = 0.989, 0.995$  and  $0.988$ ). The slopes of  $n$  were  $0.959$  for **L** with Zn(II) and  $0.995$  for **L** with Ni(II), which were both approximately equal to 1, suggesting that 1:1 metal-to-ligand complexes were formed between **L** and Zn(II) (or Ni(II)). Unlike these two ions, the slope of  $n$  for **L** and Hg(II) was  $2.022$ , which was close to 2, revealing the stoichiometric ratio of 2:1 between **L** and Hg(II). On the other hand, the association constant  $K$  could be also obtained as  $9.183 \times 10^3$  L/mol,  $2.818 \times 10^4$  L/mol and  $4.797 \times 10^9$  L<sup>2</sup>/mol<sup>2</sup> for Zn(II), Ni(II) and Hg(II) with **L**, respectively.

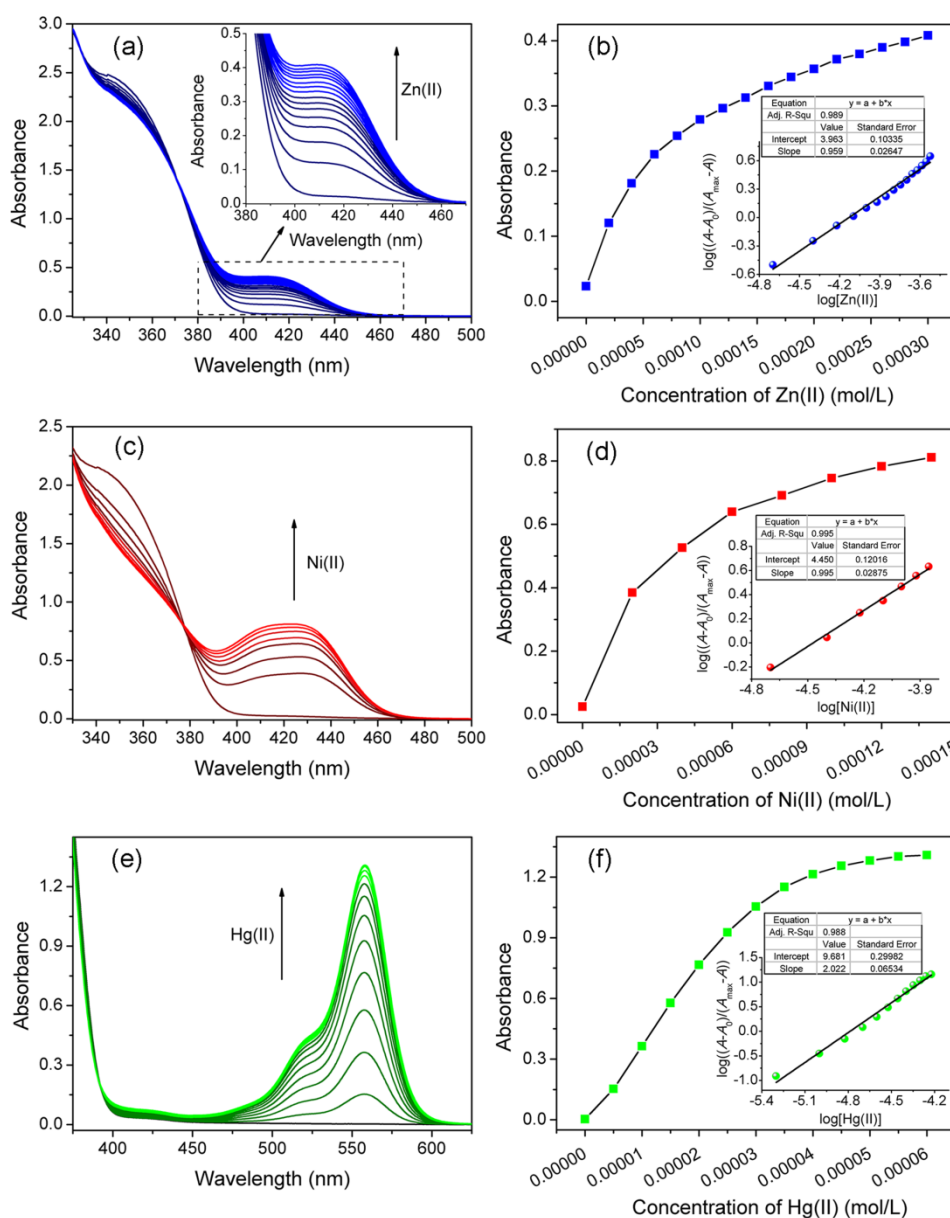


**Fig. 1.** Absorption spectra of **L** upon the addition of (a) Zn(II), (c) Ni(II) and (e) Hg(II) in

tetrahydrofuran. Absorbance at 410 nm, 421 nm and 558 nm as a function of the concentrations of (b) Zn(II), (d) Ni(II) and (f) Hg(II), respectively. Inset: linear fitting between  $\log[(A-A_0)/(A_{\max}-A)]$  and  $\log[M]$ .

Another direct evidence for the stoichiometric ratio between **L** and the metal ions were derived from ESI-MS spectra. There were peaks at  $m/z = 639.22$ ,  $633.23$  and  $1353.52$ , respectively for **L-Zn**, **L-Ni** and **L-Hg**, which corresponded well with the calculated ones ( $[\mathbf{L} + \text{Zn(II)} - \text{H}]^+$ , calcd  $639.20$ ,  $[\mathbf{L} + \text{Ni(II)} - \text{H}]^+$ , calcd  $633.20$  and  $[2\mathbf{L} + \text{Hg(II)} - \text{H}]^+$ , calcd  $1353.51$ ). All of the results verified that the stoichiometric ratios of **L** with Zn(II) and Ni(II) were both 1:1 while that of **L** with Hg(II) was 2:1.

### 3.2. Photo-induced absorbance and fluorescence change of **L** with different metal ions

The influences of metal ions on the photo-responsive behavior of **L** were first evaluated by absorption measurements of **L-M** before and after UV light irradiation. As shown in Fig. 2, both **L-Zn** and **L-Ni** showed no absorbance above 470 nm before UV light irradiation. Whereas the unirradiated **L-Hg** exhibited a weak absorbance band at about 556 nm. Interestingly, after UV light irradiation, intense absorbance peaks were induced by Zn(II) and Ni(II) around 556 nm. Meanwhile, the peak observed in the unirradiated **L-Hg** was enhanced remarkably. These absorbance changes corresponded well with the color changes observed from the photographs in Fig. 2. Before UV light irradiation, **L-Zn** was nearly colorless while **L-Ni** showed faint yellow color, which was due to the absorbance below 470 nm. **L-Hg** was pink originated from its absorbance at 556 nm. After exposure to UV light, these three complexes were all getting to deepred, which were attributed to their dominant absorbance at about 556 nm. The increased absorbance of **L-Zn**, **L-Ni** and **L-Hg** can gradually return to their originated states when the UV light was removed, which demonstrated that the photo-responsive behaviors of **L-M** were all reversible.

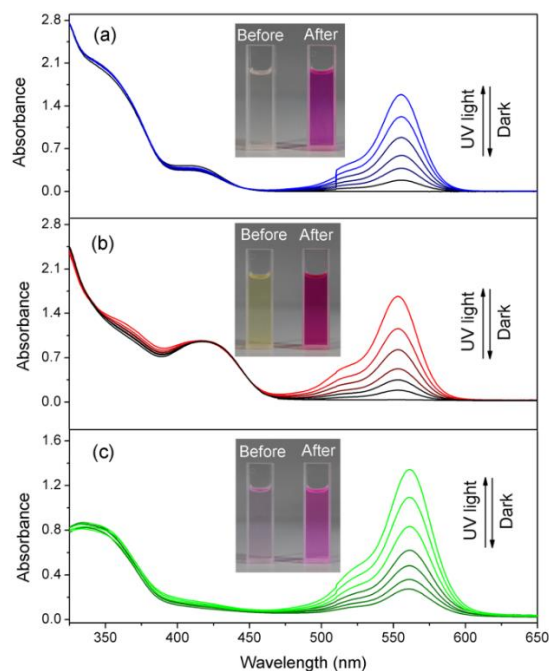


**Fig. 2.** Absorption spectra and photographs of **L** with (a) Zn(II), (b) Ni(II) and (c) Hg(II) before and after UV light irradiation.

Fluorescence measurements of **L** with Zn(II), Ni(II) and Hg(II) before and after UV light irradiation were further carried out. Interestingly, these three complexes showed totally different variation tendency. As shown in the fluorescence photographs (Fig. 3 inset), **L-Zn** emitted strong green emission and **L-Hg** showed a very weak orange emission before UV light irradiation, respectively. On the contrary, **L-Ni** was almost nonluminescent before UV light irradiation. After exposure to UV light, the emission of **L-Zn** was quenched while that of **L-Hg** enhanced. On the other hand, there was still no emission observed for **L-Ni**. To deeply investigate the fluorescence changes, their fluorescence spectra were recorded with different irradiation time. As shown in Fig. 3, there was an intense emission peak at 516 nm for unirradiated **L-Zn**. This peak split into two peaks with decreased intensities upon UV light irradiation (“turn off” mode). For **L-Hg**, the weak emission peak at 589 nm enhanced gradually with UV light irradiation time (“turn on” mode). While for **L-Ni**, no fluorescence peak can be observed regardless of whether there was UV light irradiation. As shown in Table S1, the luminescence quantum yield of **L-Zn** decreased while that of **L-Hg** increased after UV light irradiation, which were in accord with the variation trends of fluorescence intensities.

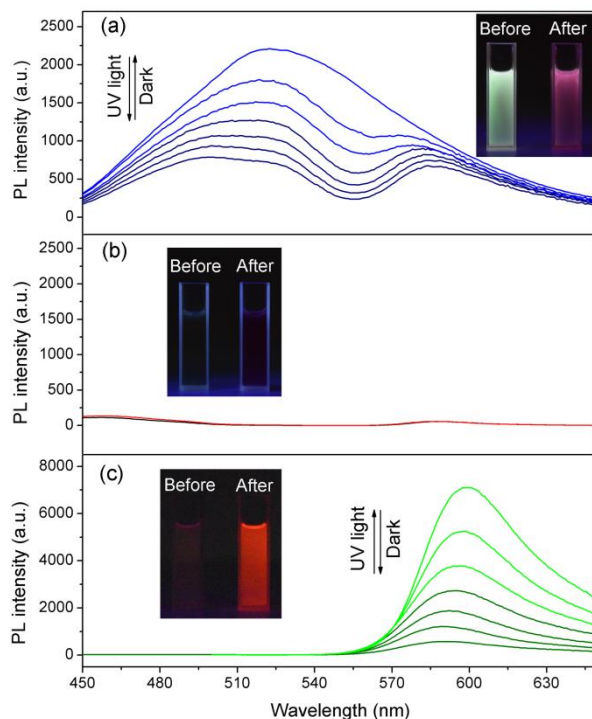
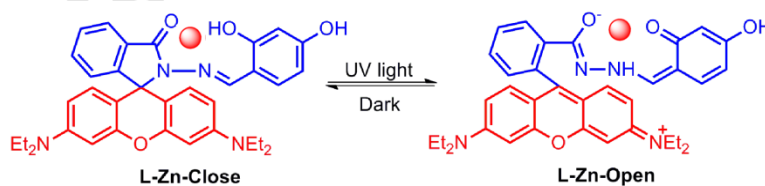


**Fig. 3.** Fluorescence spectra and photographs of **L** with (a) Zn(II), (b) Ni(II) and (c) Hg(II) before and after UV light irradiation.

According to reported literatures [31], the increased absorbance of **L** with Zn(II), Ni(II) and Hg(II) could be originated from the isomerization of the complexes (Scheme 2, take **L-Zn** as an example). After UV light irradiation, the spiro lactam ring in rhodamine B moiety turned from a close form (**L-Zn-Close**) to an open form (**L-Zn-Open**), along with enlarged conjugated structure with intense absorbance (Scheme 2, highlighted in red).



**Scheme 2.** Proposed mechanism for the isomerization of **L-Zn** upon UV light irradiation.

In order to understand the effects of metal ions on the distinctly different fluorescence response of **L-M** upon UV light irradiation, a control compound **L1** was prepared (Scheme 1). Stoichiometric ratios between metal ions and **L1** were determined by UV-vis titration experiments (Fig. S1-S3), which showed the same ratios to that between **L** and metal ions, *i.e.*, 1:1 for **L1-Zn** and **L1-Ni** while 2:1 for

**L1-Hg**. In the meantime, rhodamine B with ring-open form modulated by pH was also studied. As shown in Fig. 4(a), the fluorescence emission of **L-Zn** was similar to that of **L1-Zn** before UV light irradiation, suggesting the fluorescence of **L-Zn** was originated from the blue part showed in Scheme 2. This intense fluorescence of **L-Zn** can be attributed to the blocking effect on the photo-induced electron transfer (PET) process induced by the coordination of  $\text{Zn}^{2+}$  with nitrogen atom [37, 38]. After UV light irradiation, a valley at about 556 nm was observed in the same place of absorbance band from the UV light irradiated **L-Zn**, which was also the same absorbance peak position of rhodamine B with ring-open form (Fig. 4(b)). Meanwhile, a small valley was found at **L-Zn** around 511 nm, which was also at the un conspicuous absorbance peak position of rhodamine B. Thus, it can be determined that the quenched emission of **L-Zn** was originated from the intense self-absorption of the conjugated rhodamine B moiety. For **L-Ni**, there was no fluorescence whether or not it was irradiated because Ni(II) was paramagnetic, which always has a quenching effect on the fluorescence emission. For **L-Hg**, weak fluorescence emission at 589 nm can be observed before UV light irradiation because of the strong polarization of Hg(II), which can induce a ring open in spirolactam part. Thus, the weak fluorescence before UV light irradiation was in fact coming from that of the rhodamine B part with ring-open form (Fig. S4). After irradiated by UV light, more molecules of ring-open form were generated, resulting in a turn on fluorescence emission.

Furthermore, the fluorescence lifetimes of the complexes before and after UV light irradiation are investigated. As shown in Table S1, the fluorescence lifetimes of **L-Zn** at 516 nm before and after UV light irradiation were similar (3.64 ns and 3.65 ns, respectively), suggesting that they were originated from the same part of **1-Zn**. On the contrast, the lifetime of UV light irradiated **1-Zn** at 585 nm (2.26 ns) was different from that at 516 nm (3.65 ns), which suggested that the emission of UV irradiated **1-Zn** at 585 nm might come from another part, i.e., the rhodamine B part. The lifetimes of **L-Hg** before and after UV light irradiation were 2.44 ns and 2.02 ns, respectively, which were both close to that of **L-Zn** after UV light irradiation (2.26 ns), demonstrating these emissions were also belongs to the rhodamine B part.

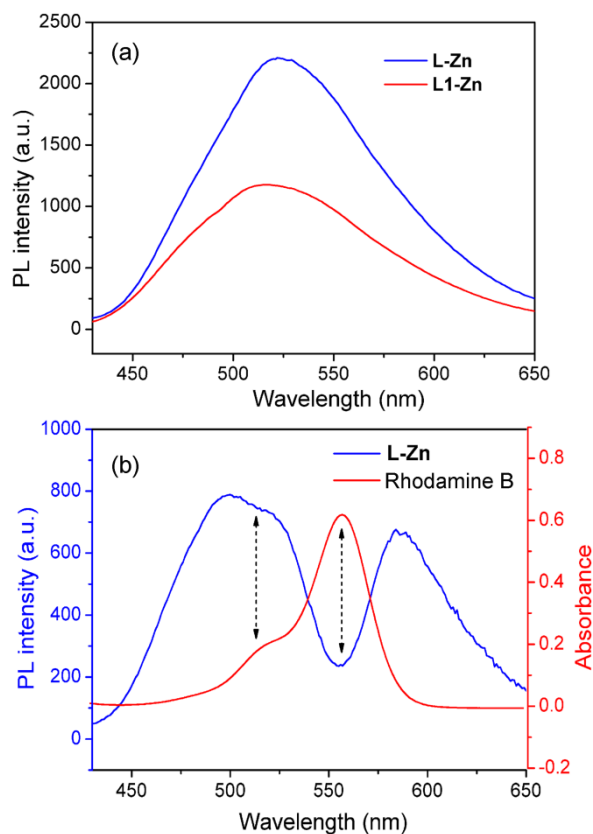


**Fig. 4.** (a) Fluorescence spectra of **L-Zn** and **L1-Zn** before UV light irradiation. (b) Fluorescence spectrum of **L-Zn** after UV light irradiation and absorption spectrum of rhodamine B with ring-open form.

### 3.3. The reversibility and fatigue resistance of L-M complexes

Besides the absorbance and fluorescence properties, the thermal bleaching kinetics of the three complexes recovered from the **L-M-Open** form to **L-M-Close** form can also be modulated by metal ions. Time dependent absorbance at 556 nm of UV light irradiated **L-M** complexes in dark was shown in Fig. 5. As shown, the recovery time of **L-Zn**, **L-Ni** and **L-Hg** was quite different, suggesting different stability of the UV light irradiated **L-M** complexes. More importantly, all of the decay curves showed excellent liner relationships between  $\ln A$  and the recovery time ( $t$ ) according to the following equation [39]:

$$\ln A = -kt \quad (2)$$

where  $A$  is the absorbance and  $k$  represents the bleaching rate constant. This liner relationship demonstrated that the recovery from **L-M-Open** form to **L-M-Close** form was a first order reaction. Meanwhile,  $k$  and half-life ( $t_{1/2}$ ) of the three

complexes could be obtained as listed in Table S2.

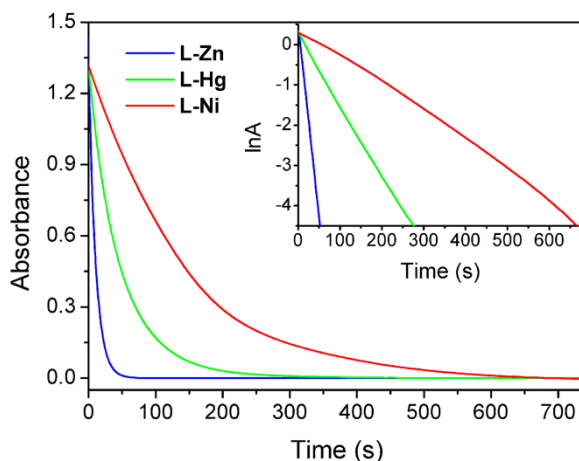


**Fig. 5.** Thermal bleaching kinetics of **L** with Zn(II), Ni(II) and Hg(II). Inset: The curves of lnA with time.

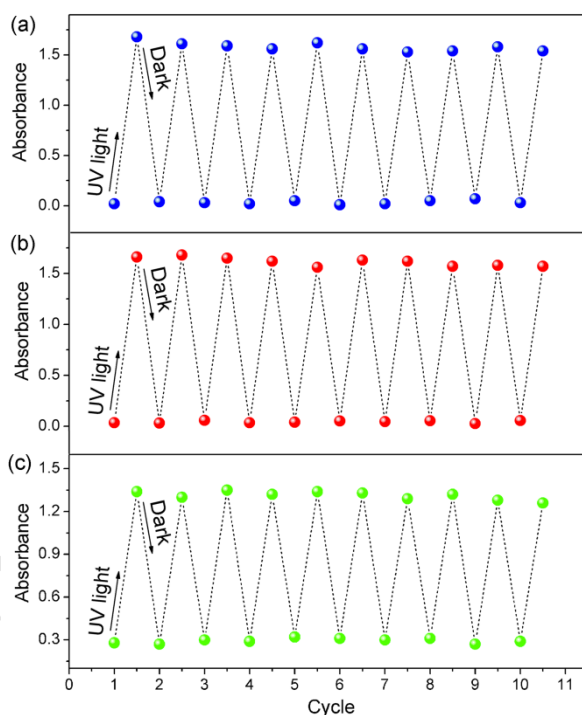


**Fig. 6.** Fatigue resistance of (a) **L-Zn**, (b) **L-Ni** and (c) **L-Hg** upon UV light irradiation and standing in dark alternately.

As reversible photo-responsive systems, the fatigue resistances of the complexes were investigated. **L-Zn**, **L-Ni** and **L-Hg** were toggled repeatedly between their **L-M-Open** form and **L-M-Close** form for 10 times. As shown in Fig. 6, the maximum absorbance at 556 nm of each complex stayed almost constant without apparent degradation even after repetition for 10 times. These results demonstrated

that all the three complexes have good fatigue resistance and excellent reversible photo-responsive properties.

### 3.4. Construction of logic gates

Inspired by the tunable fluorescence and absorbance properties of **L** by metal ions upon UV light, three logic gates could be constructed based on each individual metal ion. With respect to the inputs, the presence of Zn(II), Ni(II) or Hg(II) (In1) as well as the application of UV light irradiation (In2) were defined as “1” while their absence was “0”. The fluorescence intensity and absorbance acted as the outputs of O1 and O2, respectively. The output signals based on the fluorescence and absorbance emissions and the constructed logic gates as well as their corresponding truth tables were shown in Fig. 7. For **L** with Zn(II), fluorescence intensity at 516 nm was considered due to the turn off emission of **L-Zn** upon UV light irradiation, where the intensity of unirradiated **L-Zn** was chosen as “1” and that less than half of the originated one (the turn-off emission) was defined as “0” (Fig. 7(a)). For the output of O2, the absorbance at 556 nm was set as “1” while the absent absorbance was the “0” signal (Fig. 7(d)). As shown in Fig. 7(d) inset and Fig. 7(g), only the input with Zn(II) (In1 = 1, In2 = 0) can induce a fluorescence output signal (O1 = 1) while both the presence of Zn(II) and UV light (In1 = 1, In2 = 1) resulted in a colored state with an intense absorbance (O2 = 1). For Ni(II) with **L**, the insensitive fluorescence changes suggested that its O1 channel could be always considered as “0” (Fig. 7(b)). Nevertheless, its output of O2 with an absorbance band at 556 nm was set as “1” otherwise it was the “0” signal (Fig. 7(e)). Therefore, a logic gate with the coexistence inputs of Ni(II) and UV light (In1 = 1, In2 = 1) can induce an enhanced absorbance (O2 = 1) but other output channels were all “0”. The cases of Hg(II) with **L** were much different from the above two. On the one hand, the turn-on fluorescence intensity at 589 nm after irradiated by UV light was taken into account as its output channel of O1, with the fluorescence intensity of unirradiated **L-Hg** acting as “0” and the turn on emission as “1” (Fig. 7(c)). On the other hand, the absorbance at 556 nm was set as “1” (Fig. 7(f)). Therefore, the presence of both Hg(II) and UV light (In1 = 1, In2 = 1) resulted in the outputs of O1 = 1 and O2 = 1. The sole input of Hg(II) (In1

= 1, In2=0) can also bring an output of O2 = 1 due to its distinct absorbance with UV light irradiation. Notably, different outputs of **L** could be facily achieved by varying the metal ions coupled with UV light, which provided a simple strategy for developing photo-controlled logic gates with tunable performance.

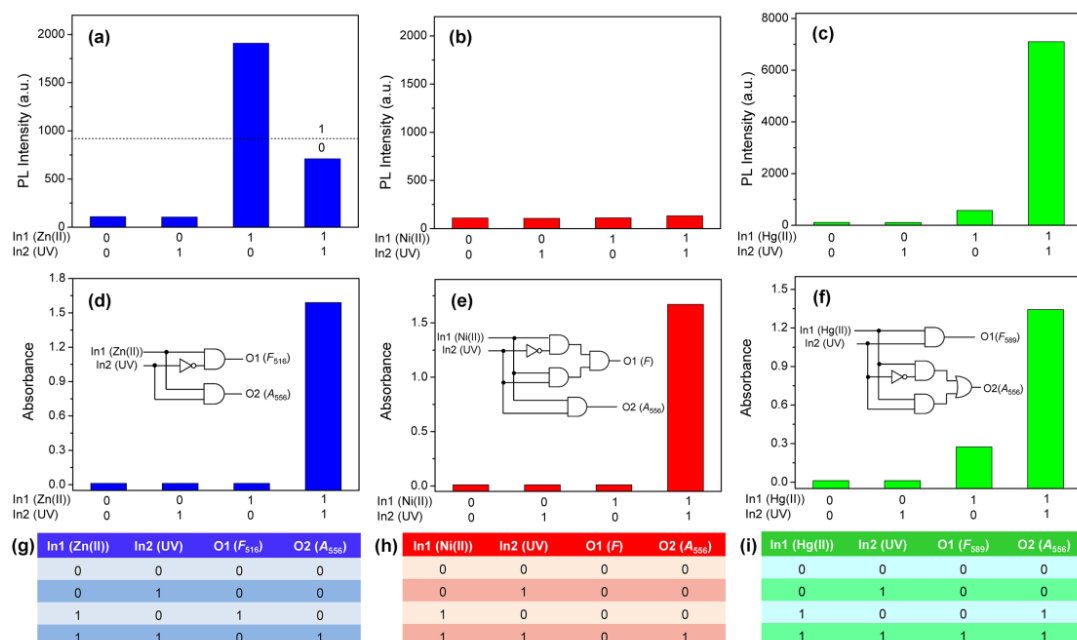


**Fig. 7.** Bar diagrams of (a)-(c) fluorescence and (d)-(f) absorbance changes upon different united inputs of metal ions and UV light irradiation. Inset: Schematic diagrams of the logic gates with different inputs. (h)-(j) The corresponding truth tables of the logic gates based on the metal ions and UV light irradiation ((a) (d) and (g) for Zn(II), (b) (e) and (h) for Ni(II), (c) (f) and (i) for Hg(II)).

## Conclusions

In conclusion, 2,4-dihydroxybenzaldehyde rhodamine B hydrazone Schiff base of **L** was prepared in this work, whose absorption and fluorescence properties as well as the thermal bleaching rate were efficiently modulated by metal ions. Stoichiometric ratios between **L** and the metal ions of Zn(II), Ni(II) and Hg(II) were 1:1, 1:1 and 2:1, respectively. Although the complexes **L-M** exhibited similar isomerization in the rhodamine B moiety from their close form to open form with enhanced absorbance, they showed entirely different photo-induced fluorescence properties upon UV light irradiation. Especially, Zn(II) induced the fluorescence of **L** from an intense emission

to two divisive quenched emissions while Hg(II) caused its fluorescence intensity from weak to pronouncedly strong after the complexes were irradiated by UV light. On the other hand, Ni(II) can not bring any fluorescence difference regardless of whether **L-Ni** was irradiated by UV light or not. Taking advantage of the prominently different characteristics caused by metal ions, different logic gates were facily designed by simply varying the inputs of metal ions and UV light. This work provided a new strategy for developing multifunctional photo-responsive materials, which were further beneficial for constructing photo-controlled logic gates with tunable performance.

### Acknowledgements

This research was supported by the foundations from National Natural Science Foundation of China (U1904172, 51502079, 21501150 and 21575034), the Training Program for Young Backbone Teachers of Henan University of Technology, the Science and Technology Key Project of Henan Education Department (18A150026), and the Open Foundation of Guangxi Key Laboratory of Processing for Non-ferrous Metals and Featured Materials, Guangxi University (2019GXYSOF12).

### References

- [1] D.-H. Qu, Q.-C. Wang, Q.-W. Zhang, X. Ma, H. Tian, Photoresponsive host-guest functional systems, *Chem. Rev.* 115 (2015) 7543-7588.
- [2] A. Fihey, A. Perrier, W.R. Browne, D. Jacquemin, Multiphotochromic molecular systems, *Chem. Soc. Rev.* 44 (2015) 3719-3759.
- [3] Y. Li, Q. Peng, S. Li, C. Yang, J. He, Q. Hu, K. Li, Facile synthesis of a photoresponsive AIEgen used for monitoring UV light and photo-patterning, *Dyes Pigments* 171 (2019) 107750.
- [4] Y. He, Y. Li, H. Su, Y. Si, Y. Liu, Q. Peng, J. He, H. Hou, K. Li, An *o*-phthalimide-based multistimuli-responsive aggregation-induced emission (AIE) system, *Mater. Chem. Front.* 3 (2019) 50-56.

- [5] K. Xu, B. Yu, Y. Li, H. Su, B. Wang, K. Sun, Y. Liu, Q. Peng, H. Hou, K. Li, Photo-induced free radical production in a tetraphenylethylene ligand-based metal-organic framework, *Chem. Commun.* 54 (2018) 12942-12945.
- [6] L. Wang, Q. Li, Photochromism into nanosystems: towards lighting up the future nanoworld, *Chem. Soc. Rev.* 47 (2018) 1044-1097.
- [7] Y. Liang, R. Wang, G. Liu, S. Pu, Effects of heteroaryl ring on the photochromism of asymmetrical diarylethenes containing a naphthalene group, *Spectrochim. Acta. A.* 205 (2018) 470-478.
- [8] L. Dong, Y. Feng, L. Wang, W. Feng, Azobenzene-based solar thermal fuels: design, properties, and applications, *Chem. Soc. Rev.* 47 (2018) 7339-7368.
- [9] R. Wang, X. Zhang, S. Pu, G. Liu, Y. Dai, Substituent effect in the photochromism of two isomeric asymmetric diarylethenes having pyrrole and thiophene units, *Spectrochim. Acta. A.* 173 (2017) 257-263.
- [10] Q. Qi, C. Li, X. Liu, S. Jiang, Z. Xu, R. Lee, M. Zhu, B. Xu, W. Tian, Solid-state photoinduced luminescence switch for advanced anticounterfeiting and super-resolution imaging applications, *J. Am. Chem. Soc.* 139 (2017) 16036-16039.
- [11] Z. Liu, H.I. Wang, A. Narita, Q. Chen, Z. Mics, D. Turchinovich, M. Kläui, M. Bonn, K. Müllen, Photoswitchable micro-supercapacitor based on a diarylethene-graphene composite film, *J. Am. Chem. Soc.* 139 (2017) 9443-9446.
- [12] L. Wang, Y. Li, X. You, K. Xu, Q. Feng, J. Wang, Y. Liu, K. Li, H. Hou, An erasable photo-patterning material based on a specially designed 4-(1,2,2-triphenylvinyl)aniline salicylaldehyde hydrazone aggregation-induced emission (AIE) molecule, *J. Mater. Chem. C* 5 (2016) 65-72.
- [13] M. Irie, T. Fukaminato, K. Matsuda, S. Kobatake, Photochromism of diarylethene molecules and crystals: Memories, switches, and actuators, *Chem. Rev.* 114 (2014) 12174-12277.

- [14] M. Kathan, P. Kovaříček, C. Jurissek, A. Senf, A. Dallmann, A. F. Thünemann, S. Hecht, Control of imine exchange kinetics with photoswitches to modulate self-healing in polysiloxane networks by light illumination, *Angew. Chem. Int. Ed.* 55 (2016) 13882-13886.
- [15] J. Zhang, Q. Zou, H. Tian, Photochromic materials: more than meets the eye, *Adv. Mater.*, 25 (2013) 378-399.
- [16] A. S. Lubbe, W. Szymanski, B. L. Feringa, Recent developments in reversible photoregulation of oligonucleotide structure and function, *Chem. Soc. Rev.*, 46 (2017) 1052-1079.
- [17] H. Qian, Y. Y. Wang, D. S. Guo, I. Aprahamian, Controlling the Isomerization Rate of an Azo-BF<sub>2</sub> Switch Using Aggregation, *J. Am. Chem. Soc.* 139 (2017) 1037-1040.
- [18] E. Hadjoudis, I. M. Mavridis, Photochromism and thermochromism of Schiff bases in the solid state: structural aspects, *Chem. Soc. Rev.* 33 (2004) 579-588.
- [19] Z. Zhou, S. Xie, X. Chen, Y. Tu, J. Xiang, J. Wang, Z. He, Z. Zeng, B. Z. Tang, Spiro-functionalized diphenylethenes: suppression of a reversible photocyclization contributes to the aggregation-induced emission effect, *J. Am. Chem. Soc.* 141 (2019) 9803-9807.
- [20] X. Wang, L. Guo, L. Feng, A multi stimuli responsive material with rhodamine B and carbazole groups, *New J. Chem.* 43 (2019) 4181-4187.
- [21] Z. Li, X. Li, H. Chen, C. He, L. Wang, Y. Yang, S. Wang, H. Guo, S.H. Liu, Multi-modulated photochromic behavior of a D-A type dithienylethene, *Dyes Pigments* 162 (2019) 712-720.
- [22] A. Li, N. Chu, L. Huang, L. Han, Y. Geng, S. Xu, L. Pan, H. Cui, W. Xu, Z. Ma, Remarkable responsive behaviors of iso-aminobenzopyranoxanthenes: protonation effect, photochromism and piezochromism, *Dyes Pigments* 162 (2019) 831-836.
- [23] K. Zheng, Q. Zou, Y. Yang, Y. Mao, J. Zhang, J. Cheng, The chromogen, structure, inspirations, and applications of a photo-, pH-, thermal-, solvent-, and

mechanical-response epoxy resin, *Ind. Eng. Chem. Res.* 57 (2018) 13283-13290.

[24] Z. Ma, Y. Ji, Y. Lan, G.-C. Kuang, X. Jia, Two novel rhodamine-based molecules with different mechanochromic and photochromic properties in solid state, *J. Mater. Chem. C* 6 (2018) 2270-2274.

[25] L. Huang, Y. Qiu, C. Wu, Z. Ma, Z. Shen, X. Jia, A multi-state fluorescent switch with multifunction of AIE, methanol-responsiveness, photochromism and mechanochromism, *J. Mater. Chem. C* 6 (2018) 10250-10255.

[26] Q. Qi, J. Qian, S. Ma, B. Xu, S.X.A. Zhang, W. Tian, Reversible multistimuli-response fluorescent switch based on tetraphenylethene-spiropyran molecules, *Chem. Eur. J.* 21 (2015) 1149-1155.

[27] J. Guo, H. Yuan, D. Jia, M. Guo, Y. Li, Synthesis and improved photochromic properties of pyrazolones in the solid state by incorporation of halogen, *Spectrochim. Acta. A.* 171 (2017) 149-154.

[28] M.-J. Liu, J. Yuan, J. Tao, Y.-Q. Zhang, C.-M. Liu, H.-Z. Kou, Rhodamine salicylaldehyde hydrazone Dy(III) complexes: Fluorescence and magnetism, *Inorg. Chem.* 57 (2018) 4061-4069.

[29] Y. Li, K. Li, B.Z. Tang, A photoactivatable photochromic system serves as a self-hidden information storage material, *Mater. Chem. Front.* 1 (2017) 2356-2359.

[30] Q. Feng, Y. Li, G. Shi, L. Wang, W. Zhang, K. Li, H. Hou, Y. Song, A photo-controllable third-order nonlinear optical (NLO) switch based on a rhodamine B salicylaldehyde hydrazone metal complex, *J. Mater. Chem. C* 4 (2016) 8552-8558.

[31] K. Li, Y. Xiang, X. Wang, J. Li, R. Hu, A. Tong, B.Z. Tang, Reversible photochromic system based on rhodamine B salicylaldehyde hydrazone metal complex, *J. Am. Chem. Soc.* 136 (2014) 1643-1649.

[32] K. Li, Y. Xiang, A. Tong, B.Z. Tang, Readily accessible rhodamine B-based photoresponsive material, *Sci. Chi. Chem.* 57 (2014) 248-251.

- [33] Z. Xu, L. Zhang, R. Guo, T. Xiang, C. Wu, Z. Zheng, F. Yang, A highly sensitive and selective colorimetric and off-on fluorescent chemosensor for  $\text{Cu}^{2+}$  based on rhodamine B derivative, *Sensors Actuators B: Chem.* 156 (2011) 546-552.
- [34] Y. Xiang, A. Tong, P. Jin, Y. Ju, New fluorescent rhodamine hydrazone chemosensor for Cu(II) with high selectivity and sensitivity, *Org. Lett.* 8 (2006) 2863-2866.
- [35] Q. Feng, Y. Li, K. Li, J. Lu, J. Wang, P. Fan, D. Li, D. Wu, H. Hou, Fluorescent chemosensor for zinc ion detection with significant emission color change in aqueous solution based on AIEgen, *ChemistrySelect* 2 (2017) 3158-3162.
- [36] M. Dong, T.-H. Ma, A.-J. Zhang, Y.-M. Dong, Y.-W. Wang, Y. Peng, A series of highly sensitive and selective fluorescent and colorimetric “off-on” chemosensors for Cu (II) based on rhodamine derivatives, *Dyes Pigments* 87 (2010) 164-172.
- [37] A. Ganguly, S. Ghosh, S. Kar, N. Guchhait, Selective fluorescence sensing of Cu(II) and Zn(II) using a simple Schiff base ligand: Naked eye detection and elucidation of photoinduced electron transfer (PET) mechanism, *Spectrochim. Acta. A.* 143 (2015) 72-80.
- [38] F. Qian, C. Zhang, Y. Zhang, W. He, X. Gao, P. Hu, Z. Guo, Visible light excitable  $\text{Zn}^{2+}$  fluorescent sensor derived from an intramolecular charge transfer fluorophore and its in vitro and in vivo application, *J. Am. Chem. Soc.* 131 (2009) 1460-1468.
- [39] Y. Li, K. Li, L. Wang, Y. He, J. He, H. Hou, B.Z. Tang, Fluoran salicylaldehyde hydrazone Zn(II) complexes: reversible photochromic systems both in solution and in a solid matrix, *J. Mater. Chem. C* 5 (2017) 7553-7560.

**Declaration of competing interests**

The authors declare that they have no known competing financial interests or personal relationships that could have appeared to influence the work reported in this paper.

The authors declare the following financial interests/personal relationships which may be considered as potential competing interests:

Journal Pre-proof

**Author Statement**

**Yuanyuan Li:** Conceptualization, Methodology, Writing-Original draft preparation, Funding acquisition.

**Zining Feng:** Data curation, Investigation.

**Yajing Li:** Investigation, Software, Validation, Data Curation.

**Wenhui Jin:** Visualization, Investigation.

**Qiuchen Peng:** Investigation, Formal analysis.

**Panke Zhang:** Conceptualization, Project administration, Writing-Reviewing and Editing.

**Juan He:** Software, Validation.

**Kai Li:** Supervision, Funding acquisition, Writing-Reviewing and Editing

Journal Pre-proof

## Graphical abstract

### Highlights

1. Photo-responsive properties of rhodamine B complexes were modulated by metal ions.
2. Spirolactam ring in rhodamine B moiety turned open upon UV light irradiation.
3. The metal ions endowed the complexes with similar photochromic property.
4. But the metal ions induced the complexes distinctly different fluorescence change.
5. Logic gates were designed by simply varying the inputs of metal ions and UV light.